



DOI: 10.18720/MCE.97.11

## Assessment of the tornado impact on the Chernobyl new safe confinement

**A.V. Perelmuter**

Scientific and Production Company «SCAD Soft» Ltd., Kiev, Ukraine

E-mail: [anatolyperelmuter@gmail.com](mailto:anatolyperelmuter@gmail.com)

**Keywords:** design-basis tornado wind speed, Fujita scale, Rankine combined vortex model, nuclear plant

**Abstract.** All the nuclear facility structures must be analyzed for tornado loads. This analysis was performed when designing the New Safe Confinement over the ruined Chernobyl power unit (NSC ChNPP). The standard methods of tornado analysis could not be applied due to its large size and geometric shape. Therefore, it was necessary to develop new calculation methods. The paper provides detailed information on the performed calculations and describes the conservative assumptions made when there was not enough information. The purpose of this paper is to analyze the gained experience of performing such an analysis of this unique structure, which may be of some interest. The following two complex problems are considered: • establishing the design tornado parameters; • developing an engineering methodology for the tornado analysis. Moreover, questions are formulated that should be clarified when carrying out similar designs.

### 1. Introduction

The recently completed New Safe Confinement of the Chernobyl Nuclear Power Plant [1, 2] is a large-scale engineering structure with a span of 257 m and a height of 108 m (Fig. 1). This structure was designed in accordance with special technical specifications which required an analysis for the possible tornado impact, and the results had to satisfy both European and national standards.

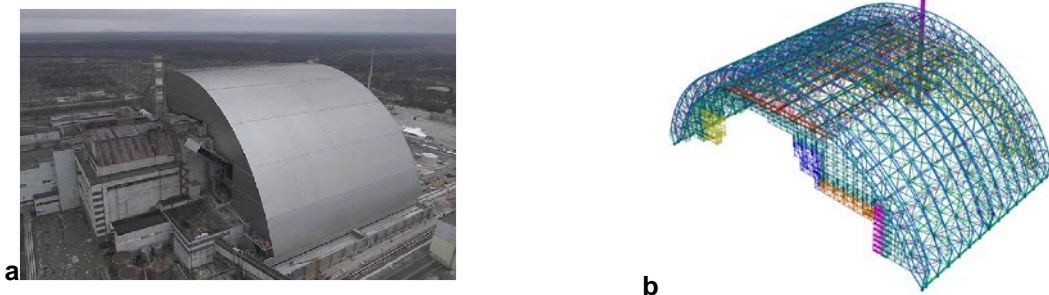


**Figure 1. The New Safe Confinement: a – general view, b – design model.**

A tornado is characterized by a vortex wind flow [3–6]. Therefore, experimental data gathered from wind tunnels generating straight-line winds could not be applied. Special laboratory wind flow simulators are used to study the tornado effect [7, 8]. However, there are only a few of them and almost all such experimental studies were performed for relatively small buildings not larger than the tornado core (see, for example [9–12]). The results of these studies could not be directly used for the considered large-scale structure as well.

The number of publications on the experience of tornado analysis of larger structures such as [13–21] is extremely small. The design data for these structures could hardly be of any use since they are specific to particular facilities with geometric configurations very different from those of the NSC ChNPP. These structures include main NPP buildings [15, 19, 20], cooling towers [21], lattice transmission towers [16, 17]. More general issues of the tornado analysis methodology considered, for example, in [4, 6, 15, 20], are closely related only to the standard main NPP buildings. Therefore, when performing the analysis for NSC ChNPP, it was necessary to postulate some characteristics of the wind flow making careful conservative decisions.



## 2. Methods

### 2.1. Expected tornado class

The safety guide [22] regulating the tornado-induced loads on nuclear facilities uses the Fujita-Pearson scale [23, 24] to classify tornadoes, which is a combination of the Fujita scale for wind speeds and the Pearson scale for path length and width.

The lower limit of Pearson path length  $L$  is:

$$L = 1.609 \times 100.5^{(k-1)}, \quad (1)$$

where  $k$  is the Fujita-Pearson scale,  $L$  is in kilometers.

The path width is the average width of the damage area measured perpendicular to the tornado path. The lower limit of Pearson path width  $W$  (in kilometers) is expressed as:

$$W = 1.609 \times 10^{0.5(k-5)}, \quad (2)$$

Unlike [22], the relationships between other tornado parameters and the tornado class were taken not discrete but continuous, as recommended in [13]. The rotational speed  $V_m$ , the translational speed of the tornado  $T$  and the pressure drop from a normal atmospheric pressure to the center of the tornado vortex  $\Delta p_X$  are defined by the  $F_k$  scale of a tornado and the following formulas:

$$V_m = 6.3(k + 2.5)^{1.5} \text{ m/sec}, \quad (3)$$

$$T = 1.575(k + 2.5)^{1.5} \text{ m/sec}, \quad (4)$$

$$\Delta p_m = 0.486(k + 2.5)^3 \text{ GPa}. \quad (5)$$

Recommendations [25] define the annual probability that a point in the local region will experience a wind speed greater than or equal to the winds in the  $F$ -scale intensity class  $k$  as the joint probability that a tornado passes through this region and its intensity is not lower than  $F_k$ :

$$P = P_S (1 - F_k). \quad (6)$$

$P_S$  is defined as the ratio of the damage area  $S$  to the product of the survey area  $A$  by the period of record  $T$ :

$$P_S = \frac{S}{A \cdot T}, \quad (7)$$

and  $F_k$  in (6) denotes the integral probability distribution function for tornadoes of various classes, which, by assumption, corresponds to an exponential law. The parameters of this distribution were determined by minimizing the standard deviation of the observed data from the specified theoretical curve.

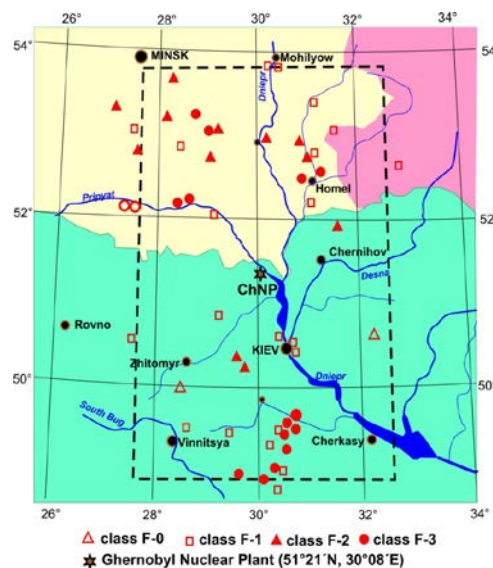


Figure 2. Map of recorded tornadoes.

According to the IAEA safety guide [22] a typical region used to evaluate the design-basis tornado is  $3^\circ$  longitude by  $3^\circ$  latitude, but the initial information for the Chernobyl NPP was taken for the  $5^\circ \times 5^\circ$  geographic square (Fig. 2). Other geographic squares were considered as well (see Table 1). After analyzing the obtained results (see Table 1), the tornado of class 3 was conservatively selected as a design action. It is characterized by the following data calculated by the formulas (3), (4) and (5):  $R_m = 59.0$  m,  $T = 20.3$  m/s,  $V_m = 81.2$  m/s,  $W = 286.1$  m.

**Table 1. The effect of the dimensions of the studied area.**

Geographic square	$2^\circ \times 2^\circ$	$3^\circ \times 3^\circ$	$4^\circ \times 4^\circ$	$5^\circ \times 5^\circ$
Damage area $S_0$ , km <sup>2</sup>	0.000	0.012	0.024	0.037
Damage area $S_1$ , km <sup>2</sup>	0.747	0.996	1.742	2.24
Damage area $S_2$ , km <sup>2</sup>	0.000	4.072	7.329	8.958
Damage area $S_3$ , km <sup>2</sup>	8.183	24.55	73.65	114.567
Total damage area $S$ , km <sup>2</sup>	8.93	29.63	82.746	125.80
Probability $P_S$ , 1/year	$6.872 \cdot 10^{-6}$	$8.03 \cdot 10^{-6}$	$1.133 \cdot 10^{-5}$	$9.86 \cdot 10^{-6}$
$F$ -class with probability $P_0 = 1 \cdot 10^{-7}$	3.32	2.79	2.86	2.90
$F$ -class with probability $P_0 = 1 \cdot 10^{-6}$	3.20	2.74	2.83	2.86
$F$ -class with probability $P_0 = 1 \cdot 10^{-5}$	–	–	2.00	–

## 2.2. Confinement load

The spatial distribution of wind speeds was taken in the form of a Rankine vortex, where the rotational speed is determined by the following formula:

$$V = \frac{r}{R_m} V_m (0 \leq r \leq R_m), \quad V = \frac{R_m}{r} V_m (R_m \leq r < \infty), \quad (8)$$

where  $V_m$  is the maximum tangential velocity;  $R_m$  is the tornado core radius with the velocity  $V_m$ .

The air rarefaction load at a point at the distance  $r$  from the tornado axis is calculated by the following formula

$$\Delta p = \frac{\Delta p_m}{2} \left( 2 - \frac{r^2}{R_m^2} \right) \quad (0 \leq r \leq R_m), \quad \Delta p = \frac{\Delta p_m}{2} \left( \frac{R_m}{r} \right)^2 \quad (R_m \leq r < \infty). \quad (9)$$

Wind velocity vector  $\vec{W}$  is the sum of vectors

$$\vec{W} = \vec{T} + \vec{V}, \quad (10)$$

where the direction of the translational velocity vector  $\vec{T}$  is constant for the entire tornado area, and the direction of the rotational velocity vector  $\vec{V}$  at each point is perpendicular to the radius  $r$  (Fig. 3).

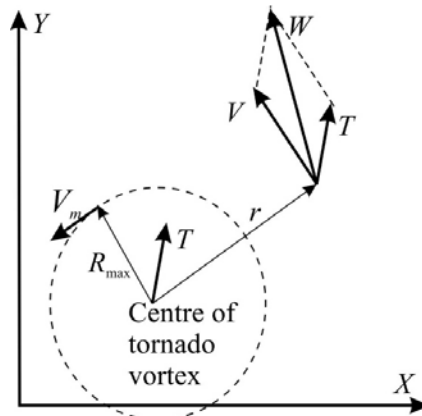


**Figure 3. Velocity components.**

Wind pressure caused by the wind velocity  $W$  is calculated by the following formula:

$$p_w = C\rho W^2 / 2 \quad (11)$$

where  $\rho = 1.22 \text{ kg/m}^3$  is the air density.

The most difficult part of the problem is to determine the drag coefficient  $C$ , which is used when calculating the velocity component of the load. Design codes and guides mainly provide information for the plane-parallel flow. The coefficients determined during the tests of the confinement model in the wind tunnel were applicable only to parallel flows and could not be used to calculate the tornado vortex effect. Therefore, it was necessary to postulate some characteristics of the wind flow making careful conservative decisions.

Thus, it was proposed to conservatively take  $C$  as one. This conservative decision  $C = 1.0$  was indirectly based on the results of the tests where the values of  $C$  were in the following range (-0.609...-1.075) for different directions of the plane-parallel flow.

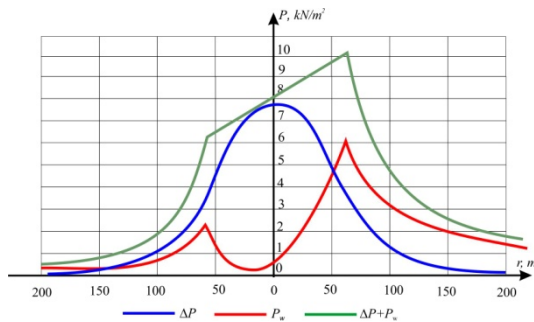


**Figure 4. Pressure distribution, line parallel to the tornado direction.**

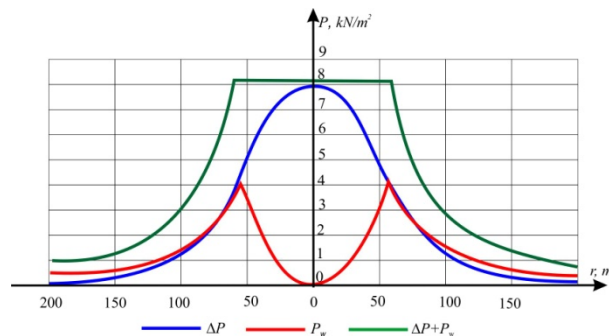


**Figure 5. Pressure distribution, line perpendicular to the tornado direction.**

Fig. 4 and 5 show the characteristic distribution of pressure along the lines parallel or perpendicular to the tornado direction:

- The red curve reflects the wind velocity pressure with a drag coefficient of 1.0, which corresponds to the main part of the roof.
- The blue curve reflects the pressure drop. This pressure is the same for all NSC enclosing structures.
- The green curve is the sum of two effects and reflects the tornado effects on the main part of the roof.

### 3. Results and Discussion

#### 3.1. Loading variants

Various tornado scenarios were considered to select load cases unfavorable for the structural members. They differ in the position of the vortex axis and the direction of translational movement. 49 different locations of the tornado axis were considered and four directions of movement were analyzed for each location of the tornado vortex (circles in Fig. 6).

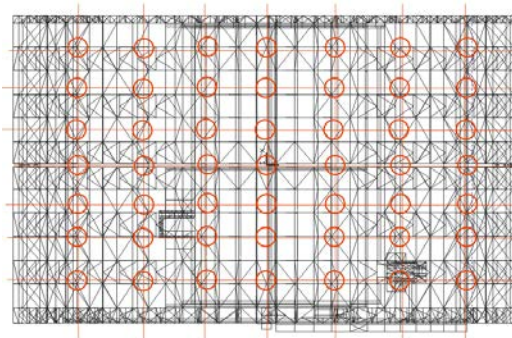


**Figure 6. Design locations of the tornado axis.**

The peak tornado-induced load reached the value of  $10.06 \text{ kN/m}^2$  and was directed upwards, i.e. against the dead load and a number of other loads. However, its unloading effect was greatly reduced due to the uneven distribution over the area, which caused significant forces in the elements of the load-bearing frame.

### 3.2. Durability check

The analysis for a tornado of class 3 was performed in accordance with the Terms of Reference assuming the integrity of the NSC sheeting:

- the tornado of class 3 was considered only in combination with permanent loads;
- the possibility of limited plastic deformations in the elements of the load-bearing structures was taken into account;
- the possible local overstress in the structural joints which did not lead to the loss of stability of the main load-bearing structures was not taken into account.

The possibility of limited plastic deformations appearance means that under a class 3.0 tornado some arch elements will have residual displacements and the estimation of their influence on the main cranes system work is required. Unfortunately, regulations (both SNiP and Eurocode) don't permit their quantitative calculation.

Anyway, the long-term practice of critical crane industrial buildings using formula (49) from SNiP II-23-81\* showed that these concerns are excessive as the field experience demonstrates that the residual deformation measured values don't obstruct the cranes work.

The results of these analyses showed that strength and stability were not provided for many elements of the preliminary NSC design. These elements are shown in red in Fig. 7.

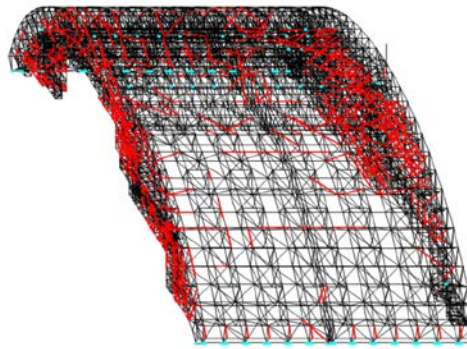


**Figure 7. Color indication of the tornado analysis results.**

New necessary cross-sections were determined to ensure compliance with the structural load-bearing capacity requirements for the tornado of class 3.0. The additional steel consumption for the new sections amounted to 344.47 tons (2.70 %).

### 3.3. Loosing contact with foundations

The bearing nodes of the arches are not capable of resisting tension, while the total lift caused by a class 3.0 tornado may achieve 20 thousand tons, the total permanent load weight being about 32 thousand tons. Therefore the hypothesis needs to be verified that some arches may break from the foundation. The hypothesis has been verified using a design model where the arch is supported by unilateral constraints.

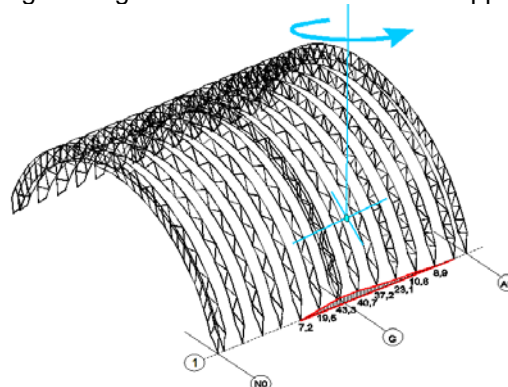


**Figure 8. Deformations in unilateral constraints.**

The respective nonlinear problem was solved by a step-by-step method in the SCAD environment. The result was refined by iteration for a few tornado load cases. Results of the check for a case which turned out to be worst from the seam opening standpoint are shown in Fig. 8.

As far as the structure of supporting node allows to provide free vertical displacements with dimension up to 50 mm with the purpose to perceive horizontal reaction components, a possibility to be found for raising by 43.3 mm is absolutely safe.

## 4. Conclusion

The experience of designing the New Safe Confinement has shown that there are a number of unresolved issues related to the methodology for determining the tornado-induced loads on large-span structures of non-standard geometric shapes. In particular, it remains unclear whether a tornado vortex can exist near a vertical wall larger than the tornado core. When designing the NSC ChNPP, we assumed that such a vortex would collapse. Issues related to the drag coefficient, which is used to determine the vortex pressure on the enclosing structures, require clarification and can initiate further studies.

It should also be noted that the methodology for determining the expected tornado class has to be refined. The applied approach, which was based on the IAEA recommendations, does not take into account the local features of the construction site, and therefore can lead to incorrect results.

## References

1. Wastiaux, M., Etienne, D. Arche de Tchernobyl: Un ouvrage metallique de duree 100 ans sana maintenance [Online]. URL: <http://afgc.asso.fr/images/stories/visites/GC2011/Session1-7-Wastiaux-Etienne-Tchernobyl.pdf> (reference data 04.02.2020)
2. Boutillon, L., Coulet, D., Waustiaux, M. The Chernobyl new safe confinement: an exemplary contribution by french companies. The French Technology and know-how. Document issued at the 19<sup>th</sup> IABSE Congress in Stockholm. Sweden September 21–23, 2016. [Online]. URL: <http://www.afgc.asso.fr/images/stories/pub/Stockholm/18-The-Chernobyl-new-safe-confinement-an-exemplary-contribution-by-french-companies.pdf> (reference data 04.02.2020)
3. Solari, G. Wind Science and Engineering. Origins, Developments, Fundamentals and Advancements Springer Nature Switzerland AG, 2019. 944 p. <https://doi.org/10.1007/978-3-030-18815-3>
4. Simiu E., Dong, Hun Yeo. Wind Effects on Structures: Modern Structural Design for Wind, John Wiley & Sons, 2019/ 520 p. DOI: 10.1002/9781119375890
5. Gordeev, V.N., Lantuh-Lyaschenko, A.I., et al. Nagruzki i vozdeystviya na zdaniya i sooruzheniya [Loadings and actions on buildings and constructions]— Moscow: Izd-vo SKAD SOFT, Izd-vo Assotsiatsii stroitelnyih vuzov, DMK Press, 2017. 588 p. (rus)
6. Birbraer, A.N., Roleder, A.J. Extreme actions on structures. Saint Petersburg: Polytrchnic University Publisher House, 2009. 594 p. (rus.)
7. Jischke, M.C., Light, B.D. Laboratory simulation of tornadic wind loads on a rectangular model structure. Journal of Wind Engineering and Industrial Aerodynamics. 1983. Pp. 371–382. DOI.org/10.1016/0167-6105(83)90157-5
8. Sarkar, P., Haan, F., Gallus, Jr.W., et al. Velocity measurements in a laboratory tornado simulator and their comparison with numerical and fullscale data. Technical Memorandum of Public Works Research Institute. 2005. Pp. 197–211. [Online]. URL: <https://www.pwri.go.jp/eng/ujnr/joint/37/paper/42sarkar.pdf> (reference data 04.02.2020).
9. Balaramudu, V. Tornado-induced wind loads on a low-rise building. Retrospective Theses and Dissertations. 2007. <https://lib.dr.iastate.edu/rtd/14860>
10. Case, J., Sarkar, P., Sritharan, S. Effect of low-rise building geometry on tornado-induced loads. Journal of Wind Engineering and Industrial Aerodynamics. 2014. Vol.133, Pp. 124–134. DOI: 10.1016/j.jweia.2014.02.001
11. Zhenqing, L., Takeshi, I. A study of tornado induced mean aerodynamic forces on a gable-roofed building by the large eddy simulations. Journal of Wind Engineering & Industrial Aerodynamics. 2015. Vol. 146. Pp. 39–50. <https://doi.org/10.1016/j.jweia.2015.08.002>
12. Xua, F., Maa, J., Chenb, W.-L., Xiaoa, Y.-Q., Duan, Z.-D. Analysis of load characteristics and responses of low-rise building undertornado. Procedia Engineering. 2017. Vol. 210. Pp. 165–172. <https://doi.org/10.1016/j.proeng.2017.11.062>
13. Wen, J.-K. Dynamic tornado wind loads on tail buildings. Journal of the Structural Division. Proc. ASCE. 1975. — ST1, Pp. 169–182.
14. James, A. Dunlap. Nuclear Power Plant Tornado Design Considerations. Journal of the Power Division. 1971. 97 (2). Pp. 407–417. [Online]. URL: <https://cedb.asce.org/CEDBsearch/record.jsp?dockey=0018118> (reference data 04.02.2020)
15. Barrett, D.J., Agarwal, R., Persinko, D. The effect of a tornado on nuclear power plant structures. Transactions of the 7 international conference on structural mechanics in reactor technology. Vol. D Netherlands: North-Holland, 1983, Pp. 243–249.
16. Ahmad, S., Ansari, Md.E. Response of transmission towers subjected to tornado loads. The Seventh Asia-Pacific Conference on Wind Engineering. 2009. [Online]. URL: [https://www.researchgate.net/publication/228790798\\_Response\\_of\\_transmission\\_towers\\_subjected\\_to\\_tornado\\_loads/stats](https://www.researchgate.net/publication/228790798_Response_of_transmission_towers_subjected_to_tornado_loads/stats) (reference data 04.02.2020)
17. Savory, E., Gerard, A.R., Zeinoddini, M., Toy, N., Disney, P. Modeling of Tornado and Microburst Induced Wind Loading and Failure of a Lattice Transmission Tower. Engineering Structures. 2001, Vol.23. Pp. 365–375.
18. Selvam, R.P., Millett, P.C. Computer modeling of tornado forces on buildings. Wind and Structures. 2003, 6(3). 3 Pp. 209–220. DOI: 10.12989/was.2003.6.3.209
19. Kozlov, I.L. Criteria for NPP industrial site flooding by combined impact of tornadoes and earth-quakes in the cooling pond. Eastern-European Journal of Enterprise Technologies. 2015, Vol. 3, No. 6 (75). DOI: <https://doi.org/10.15587/1729-4061.2015.42146>
20. Biswas, J. Tornado Generated Missile Impact to NPP Structures. ASCE Structures Congress 2019. Orlando, Florida. DOI.org/10.1061/9780784482230.031
21. Bazhenov, V.A., Huliar, A.I., Snizhko, N.A., Ovsianikov, O.S. Raschet gradirni AES na vitrovye nagruzki tipa «tornado» poluanaliticheskim metodom konechnyx elementov. [Cooling tower of the atomic power station calculation on wind loadings of type of a tornado a semi-analytical method of finite elements] Opir materialiv i teoriia sporud [Strength of materials and the theory of constructions]. № 71. 2002. Pp. 3–11. (ukr)
22. IEFA Safety Standards Series. Safety Guide 50-SG-S11A. Extreme Meteorological Events in Nuclear Power Plant Siting, Excluding Tropical Cyclones. A Safety Guide, International Atomic Energy Agency: Vienna. 1981. 76 p.
23. Fujita T.T. Tornadoes and downbursts in the context of generalized planetary scales Journal of Atmospheric Sciences, 1981, 38 (6). Pp. 1511–1534.
24. Fujita, T.T., Pearson, A.D. Results of FPP Classification of 1971 and 1972 Tornadoes. Propertis of 8<sup>th</sup> Conference on Severe Local Storms. 1973. Boston, Massachusetts (1973).
25. Rekomendatsii po otsenke kharakteristik smercha dlya ob'ektov ispol'zovaniya atomnoy energii [Recommendations for assessing the characteristics of a tornado for nuclear facilities. Rukovodstva po bezopasnosti RB-022-01. Gosatomnadzor Rossii. 2002. 69 p.

## Contacts:

Anatoly Perelmuter, [anatolyperelmuter@gmail.com](mailto:anatolyperelmuter@gmail.com)

© Perelmuter, A.V., 2020